KINETIC ANALYSIS OF FLASH PHOTOLYSIS DATA FOR SEQUENTIAL FIRST AND SECOND ORDER REACTIONS: THE PHOTOREDUCTION OF TRIPLET FLUORENONE BY DABCO

LEONARD J. ANDREWS*, JOEL M. LEVY and HENRY LINSCHITZ

*Department of Chemistry, Brandeis University, Waltham, Massachusetts 02154 (U.S.A.)*

(Received September 1, 1976; in revised form November 2, 1976)

Summary

In studying reactions of triplet states by flash photolysis, particularly with laser techniques, one frequently encounters the kinetic problem of an initial pseudo-first order triplet reaction overlaid by a second order decay of products. A simple algorithm is given, adaptable to a desk-top calculator, for treatment of experimental data to obtain rate constants and total product yields (or absorptions) in this situation. The procedure is illustrated in the case of the photoreduction of fluorenone triplet by 1,4-diazabicyclo(2.2.2) octane, a reaction which yields a pair of radical-ions.

Introduction

A kinetic problem frequently arises in solution flash photolysis when the pseudo-first order growth of a reaction product is overlapped by its simultaneous second order decay. A familiar photochemical example is the reaction of a triplet molecule with a redox reagent, by hydrogen atom or electron transfer, to produce two radicals or radical-ions, which then decay by recombination or dismutation. Thus, for a triplet acceptor reacting with a donor in polar media, we have:

$$^3A + B \xrightarrow{k_R} A^- + B^+$$

$$A^- + B^+ \xrightarrow{k_2} A + B$$
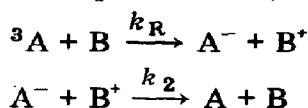
Another example, involving energy transfer from a triplet, is the pseudo-first order growth of an acceptor triplet overlapped by its bimolecular annihilation [1]. If the overlap of the first and second order process is appreciable, it becomes quite awkward to determine accurately such important parameters of the situation as the initial reaction rate constant and the total product yield. The latter quantity is of special interest if the initial reaction with B is accompanied by a competing process leading directly to the ground state (quenching).

*Present address: GTE Laboratories, Inc., Waltham, Mass. 02154 (U.S.A.).

In principle, the pseudo-first order growth and second order decay processes can, of course, be separated by decreasing the flash intensity or triplet precursor concentration, perhaps with a concurrent increase in path length [2]. However, the extent to which this can be done, consistent with acceptable experimental error in measuring the transient absorption, depends on several factors, including the spectra and extinction coefficients of the ground state and transient species, the values of the rate constants and even the experimenter's patience in removing quenching impurities and oxygen from large volumes of solution. The rapidly increasing use of pulsed laser sources in flash photolysis studies makes the kinetic problem particularly pertinent. The short time resolution (~ 50 ns) afforded by Q-switched lasers makes it possible to work at such high reagent (or quencher) concentrations that the triplet lifetime is controlled essentially by the pseudo-first order reaction. Thus, kinetic complications caused by the competing second-order triplet annihilation process [3] are conveniently avoided. At the same time the small cross-section of the laser beam and resulting high concentration of reaction products promotes their bimolecular decay. In the frequently encountered case where an exponentially falling triplet absorption overlaps a hyperbolic radical decay (see Fig. 1(b) below), accurate kinetic analysis becomes particularly troublesome.

In this paper we present a simple algorithm, requiring only a desk-top calculator, to determine the primary rate constant and total product absorption in the above kinetic situation. The method is especially well adapted to flash procedures utilizing Q-switched lasers.

Kinetic models and procedure

To provide a quantitative "feel" for the problem, we illustrate the kinetic situation with simulated flash photolysis data in which absorbance changes (ΔD_t) following excitation are monitored at an appropriate wavelength. We assume a rather fast ($k_R = 10^8$ M^{-1} s^{-1}) reaction between a triplet species and reagent, B, which in presence of excess B (10^{-2} M) becomes pseudo-first order ($k_1 = 10^6$ s^{-1}). We assume further that the products decay bimolecularly at a diffusion-controlled rate ($k_2 = 10^{10}$ M^{-1} s^{-1}), and that the flash duration and triplet formation are instantaneous. In Fig. 1(a), the monitoring wavelength is taken such that the extinction coefficient of the product is twice that of the parent triplet. The product "half-life" ($\sim 1/k_2 T_0$) is then controlled by varying the initial triplet concentration, T_0, corresponding to initial absorption, ΔD_0. For the conditions given in Fig. 1(a), this "half-life" spans the range 5 μs to 1 ms. At $\Delta D_0 = 5 \times 10^{-4}$ or $T_0 = 1.0 \times 10^{-7}$ M, the product appearance is essentially exponential and the experimental absorbance time curve has a good, flat maximum (ΔD_∞). The rate constant for product growth is given by the slope of $\ln(\Delta D_\infty - \Delta D_t)$ vs. time, and the density corresponding to total yield is directly accessible from the data. At higher ΔD_0 values, this simple treatment is no longer adequate. Thus (Fig. 1a)
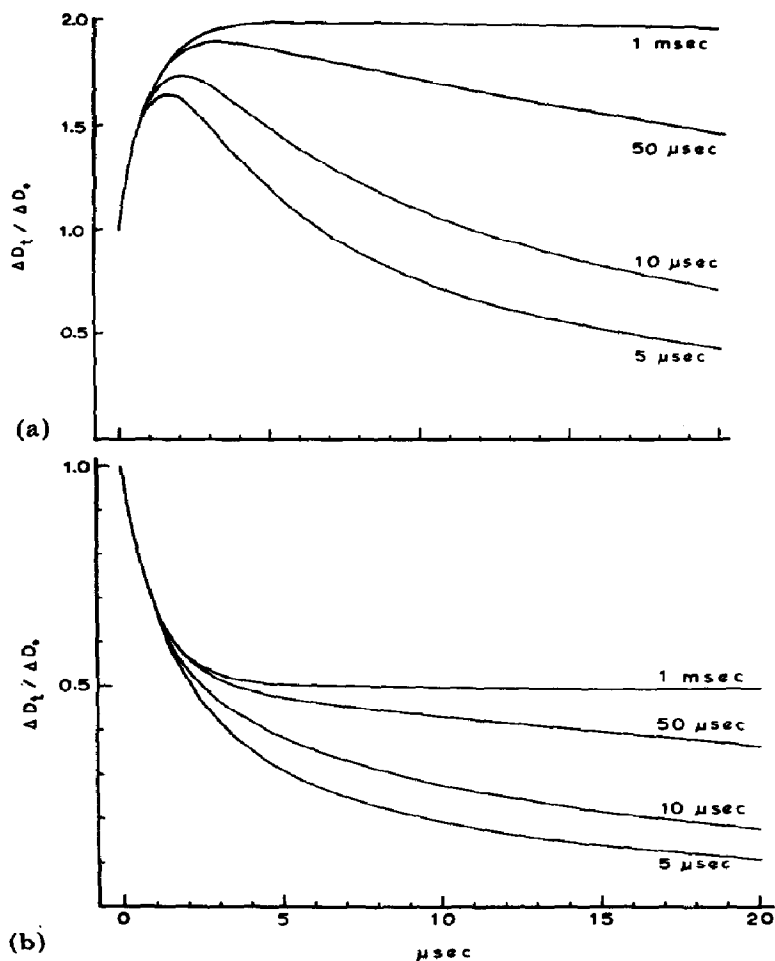
Fig. 1. Flash photolysis data simulated using eqn. (4). $k_1 = 10^6$ s^{-1}, $k_2 = 10^{10}$ M^{-1} s^{-1}, $\Delta\epsilon_R = 10^4$ M^{-1} cm^{-1}, cell path = 1 cm. (a) $\Delta\epsilon_R/\Delta\epsilon_T = 2$; $\Delta D_0^T = 0.0005, 0.01, 0.05, 0.1$. (b) $\Delta\epsilon_R/\Delta\epsilon_T = 0.5$; $\Delta D_0^T = 0.002, 0.04, 0.2, 0.4$. Indicated second order "half-lives" = $1/k_2 T_0$.

at ΔD_0 as low as 0.01 ($T_0 = 2 \times 10^{-6}$ M), the overlap of product growth and decay is already noticeable. In the region where signal/noise considerations require data to be taken, the maximum in the transient absorbance curve cannot serve as a basis for obtaining k_1 and gives only a lower limit for the total product yield (or absorption). Figure 1(b) presents the situation in the same range of initial triplet concentration (product half-life) as in Fig. 1(a), but taking a wavelength where the triplet extinction coefficient is twice that of the reaction product. Again, it is only in the limit of impractically small ΔD values that simple kinetic analysis is applicable.

A straightforward but computationally tedious solution to this problem involves numerical integration of the non-linear rate law corresponding to the reaction mechanism. We have developed an alternative, much simpler procedure, to deal with the specific kinetic problem discussed above.

If the product concentration–time profile is divided into a large number of channels of equal width, Δt, then the product concentration in the nth channel (*i.e.*, at time $n\Delta t$) is given approximately (see Appendix) by:

$$R_n = \alpha T_0 [e^{-(n-1)k_1\Delta t} - e^{-nk_1\Delta t}] + R_{n-1}/(1 + R_{n-1}k_2\Delta t) \tag{1}$$

where $n \geqslant 1$, $R_0 = 0$, T_0 is the initial triplet concentration, k_1 is the pseudo-first order rate constant for triplet reaction with excess reagent ($k_1 = k_R B$), k_2 is the second order rate constant for product disappearance and α is the product yield. The first term in eqn. (1) gives the concentration of product formed from triplet during the interval Δt between channel $(n-1)$ and channel n and the second term gives the concentration of product remaining from channel $(n-1)$ after it has undergone second order decay for a time Δt. In the usual experimental circumstances, product formation is faster than product decay, *i.e.* $k_1 > k_2 T_0$. For this condition, two limiting cases of eqn. (1) are of interest.

If $k_2 = 0$, eqn. (1) reduces to:

$$R_n = \alpha T_0 (1 - e^{-nk_1\Delta t}) \tag{2}$$

representing simple exponential growth in the absence of decay.

If $n\Delta t \gg k_1^{-1}$, representing the time regime where product formation is complete, eqn. (1) becomes:

$$R_n = R_{n-1}/(1 + R_{n-1}k_2\Delta t) \tag{3}$$

which is a recursion form of the second order rate law. Thus eqn. (1) assumes the correct analytical forms in these two limits.

We now write eqn. (1) in terms of the observed quantity ΔD, recognizing that, in general, triplet absorption at the monitoring wavelength is not negligible. Thus:

$$
\begin{aligned}
\Delta D_n &= \Delta\epsilon_T T_n + \Delta\epsilon_R R_n \\
&= \Delta D_n^T + \Delta D_n^R \\
&= \Delta D_0^T e^{-nk_1\Delta t} + \Delta D_\infty^R (e^{-(n-1)k_1\Delta t} - e^{-nk_1\Delta t}) + \\
&\quad \Delta D_{n-1}^R/(1 + \Delta D_{n-1}^R k_2'\Delta t)
\end{aligned}
\tag{4}
$$

with $n \geqslant 1$, $\Delta D_0^R = 0$ and $\Delta D_0 = \Delta D_0^T$.

In eqn. (4), the contribution of each species is explicitly denoted: k_2 is replaced by $k_2' = k_2/\Delta\epsilon_R$; $\Delta D_0^T = \Delta\epsilon_T T_0$ is the initial triplet absorption; $\Delta D_\infty^R = \alpha T_0 \Delta\epsilon_R$ is the final product absorbance which would be observed in the *absence* of product decay; $\Delta\epsilon_T$ and $\Delta\epsilon_R$ are the differences in extinction coefficient between the triplet and product respectively and the original ground state precursor. For simplicity, we assume that the reagent B does not absorb at the monitoring wavelength and the path length is 1 cm.

In applying eqn. (4), ΔD_0^T is obtained directly from the data and k_2' from the limiting slope of ΔD^{-1} *vs.* time. Using these parameters and a sufficiently small Δt interval, and assuming values of k_1 and ΔD_∞^R, the sequence of ΔD_n values is then computed by recursion, starting with ΔD_0. The values of k_1 and

ΔD_{∞}^{R} are then varied to give the best least squares agreement with the experimental ΔD_{n} values. The search for the best k_{1} and ΔD_{∞}^{R} is greatly facilitated by initial estimates of these constants based on the experimental transient absorbance–time data. In practice, by judicious adjustment of experimental conditions (particularly reagent concentration) to optimize the difference between product growth and decay, we find that k_{1} can often be estimated to within a factor of two, and ΔD_{∞}^{R} within 20%.

A simple grid search procedure was adopted in which all combinations of the parameters k_{1}, $k_{1} \pm 20\%$, $k_{1} \pm 40\%$ and ΔD_{∞}^{R}, $\Delta D_{\infty}^{R} \pm 5\%$ and $\Delta D_{\infty}^{R} \pm 10\%$ are tested. If the best fit is found to lie at an extremum of this initial grid, the choices of k_{1} and ΔD_{∞}^{R} are revised and the coarse grid search repeated. Otherwise, the search is continued for two subsequent cycles, reducing the grid interval by a factor of three for each cycle. Thus, a minimum of 75 pairs of k_{1}, ΔD_{∞}^{R} values are searched, with final grid increments of $k_{1}/45$ and $\Delta D_{\infty}^{R}/180$. This concise search procedure is possible first, because the error surface in the vicinity of the best fitting values of k_{1} and ΔD_{∞}^{R} shows no local minima (see Fig. 4 below) and second, because good initial estimates of these parameters can be obtained directly from the experimental data.

To demonstrate the above procedure, we present results obtained in a recent study of the reaction of triplet fluorenone and amines [4]. In acetonitrile solution, using the amine 1,4-diazabicyclo(2.2.2)octane (DABCO), this reaction follows the simple reversible electron transfer mechanism written earlier. Figure 2 shows laser flash data taken on this system at the absorption maxima respectively of fluorenone radical anion (540 nm), and fluorenone triplet (425 mm). The form of the data indicates that both triplet decay and anion growth are overlapped by anion decay. The calculated best fit to the data, using eqn. (4) is shown as the solid lines in Fig. 2, obtained with $k_{1} = 6.1 \times 10^{5}$ s^{-1} at 540 nm and 6.7×10^{5} s^{-1} at 425 nm. Evaluating k_{1} in this way over a range of DABCO concentrations, gives the results summarized in Fig. 3. The excellent linearity and zero intercept of the plot provide good evidence that the radical anion is a primary product of the triplet–amine reaction. The slope of the line corresponds to the rate constant $k_{R} = 7.2 \times 10^{9}$ M^{-1} s^{-1}.

Under conditions such that reaction with DABCO represents the exclusive triplet decay path, $\Delta D_{\infty}^{R}/\Delta D_{0}^{T} = \alpha \Delta \epsilon_{R}/\Delta \epsilon_{T}$. Since it is useful to compare the absorptions of product and triplet at their respective maxima, ΔD_{∞}^{R} obtained by fitting the data at 540 nm is combined with ΔD_{0}^{T} measured at 425 nm in a separate experiment, performed under identical conditions of concentration and flash energy. This ratio is listed in Fig. 3 along with the ratio of absorbances measured at 425 nm for both species. It is found that, in polar solvents, this ratio is constant for a series of reductants (DABCO, triethylamine, dimethylaniline), strongly implying that $\alpha = 1$ in all these cases.

The criterion of best fit in applying eqn. (4) is minimum χ^{2}, which is defined as the sum of unweighted squared deviations between calculated and experimental ΔD values. It is instructive to investigate the behavior of χ^{2} in the vicinity of the best fitted k_{1} and ΔD_{∞}^{R} values in order to assess the pre-
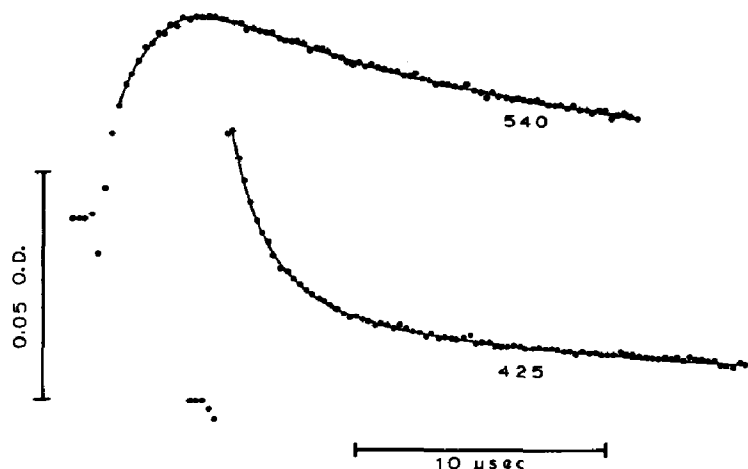
Fig. 2. Laser flash data taken at 425 and 540 nm with fluorenone $(10^{-3} M)$ and DABCO $(10^{-4} M)$ in acetonitrile. Cell path is 2.5 cm. $\lambda = 540$ nm: $k_1 = 6.1 \times 10^5 \, s^{-1}$; $\Delta D_\infty^R = 0.0520$; 425 nm: $k_1 = 6.7 \times 10^5 \, s^{-1}$, $\Delta D_\infty^R = 0.0208$. The maximum observed ΔD at 540 nm is 0.044. Δt (channel width) = 0.25 μs.
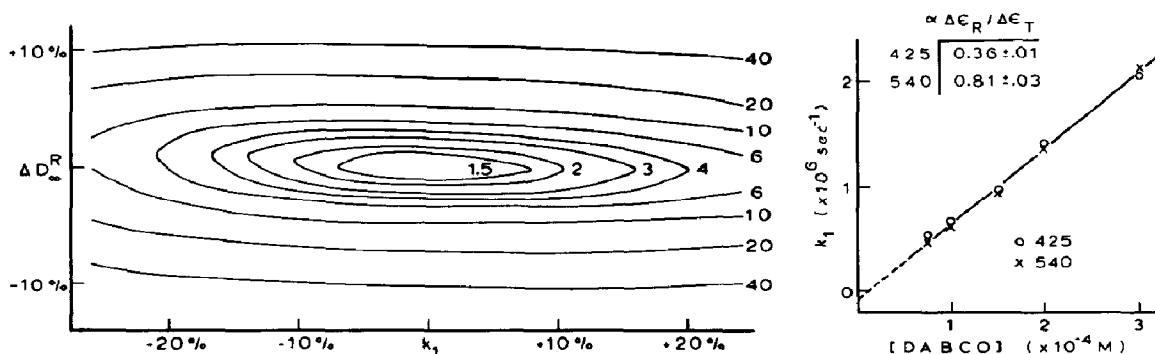

Fig. 3. Dependence of k_1 on DABCO concentration at 540 and 425 nm. Bimolecular quenching rate constant is $7.2 \times 10^9 \, M^{-1} \, s^{-1}$. See text for definition of $\alpha \Delta \epsilon_R / \Delta \epsilon_T$.

Fig. 4. Contours of constant χ^2 are shown for the 540 nm data in Fig. 2. Axes are $k_1 + k_1/10$, $k_1 \pm k_1/5$, etc.; χ^2 values are in units of 10^{-5} with the best fit value equal to 1.01 $\times 10^{-5}$.

cision attributable to the fitted parameters. Figure 4 presents contours of constant χ^2 for the 540 nm data in Fig. 2. Note that a variation of ±5% from the best value for ΔD_∞^R increases χ^2 by a factor of ten, whereas the same relative variation in k_1 increases χ^2 by less than 50%. Clearly, the sensitivity of the fit to ΔD_∞^R permits a high degree of confidence to be placed in the precision of this parameter, whereas a somewhat greater uncertainty must be tolerated for k_1.

The effect of channel width on k_1 and ΔD_∞^R is investigated in Table 1, for an experimental situation similar to that of Fig. 2(a). A single flash photolysis trace (consisting of 800 digital readout values from the transient recor-

TABLE 1

Reaction of fluorenone triplet with DABCO in acetonitrile; effect of channel width, Δt, on kinetic analysis

Δt (μs)	No. of channels n	ΔD_0	$\tau_1/\Delta t$	$k_1 \times 10^5$ (s^{-1})	ΔD_∞^R
0.50	16	0.0468	3.6	5.8	0.114
0.25	32	0.0412	7.2	5.7	0.117
0.15	53	0.0363	12.0	5.6	0.119
0.10	80	0.0319	18.0	5.7	0.121
0.07	114	0.0322	25.7	5.7	0.121

[Fluorenone] = $1.5 \times 10^{-3}\,M$; [DABCO] = $7.5 \times 10^{-4}\,M$; λ = 540 nm; detection RC = 0.035 μs; τ_1 = 1.8 μs; cell path = 2.5 cm; ΔD_{max} (observed) = 0.092; k_2' = $1.01 \times 10^6\,s^{-1}$.

der, over 8 μs) was analyzed, varying the channel width from 0.5 to 0.07 μs. The ΔD_n values used in the computation were averages of the sampling readings within each Δt interval. (In experiments where ΔD_t is read from photographic oscillogram projections, ΔD_n values will, of course, be taken from smoothed curves drawn through the trace.) The period fitted (8 μs) corresponds in this case to 4.5 triplet lifetimes. It is seen that, except for the coarsest time resolution (0.50 μs), the fitted parameters are essentially independent of Δt. This result has important practical consequences if a slow calculator is used for the fitting procedure. Our program on the HP-9821A machine requires 0.228 s/channel to compute a decay curve, or 11.4 min to fit a 40 channel transient curve after 75 iterations. Table 1 shows further that, for the given conditions, the observed ΔD_{max} (0.092) of the reaction product is about 25% less than the absorbance corresponding to the total product actually formed in the reaction (ΔD_∞^R = 0.121).

The fixed input parameter ΔD_0 necessary in the fitting routine requires further comment. Although ΔD_0 is simply the first data point on the experimental curve to be analyzed, it is sensitive to instrumental artifacts and care should be exercised to mitigate distortion. Thus scattered light from prompt fluorescence and the excitation flash should be minimized and the detection bandwidth should be as high as practicable. We normally use a detection RC time constant of 0.035 μs to acquire data for which $1/k_1 \sim 1\ \mu s$. Fortunately, the data treatment itself provides an internal check or indication of such error in ΔD_0, in the form of *systematic* deviations between the calculated and experimental points. For example, too low a ΔD_0 value gives a computed "best" transient curve which initially lies below and finally above the experimental curve. Too high a ΔD_0 value gives the reverse effect. It is helpful to arrange the form of the computation so as to indicate the presence of such correlated errors. However, in the absence of instrumental artifacts, it is our experience that taking an average "ΔD_0" over the initial Δt increment gives good results. This is seen in Table 1, which lists the values of ΔD_0 used for each calculation. The "ΔD_0" values vary quite widely, moving along the

TABLE 2

Effect of number of points, n, on kinetic analysis

Channels n	$n\Delta t/\tau_1$	$k_1 \times 10^5$ (s^{-1})	ΔD_∞^R
24	2.0	6.3	0.115
36	3.0	5.7	0.119
48	4.0	5.7	0.119
60	5.0	5.7	0.119

Δt = 0.15 μs; other conditions as in Table 1.

rising transient curve as Δt becomes larger. Nevertheless, as long as the average "ΔD_0" lies on the transient, reasonably near the origin, the search procedure gives k_1 and ΔD_∞ values which are surprisingly insensitive to the actual ΔD_0 value used.

Finally, Table 2 illustrates the effect of varying total number of channels, n, at Δt = 0.15 μs for the data analyzed in Table 1. As is indicated in Table 2, it has been our experience that systematic errors arise if decay curves are fitted over too few triplet lifetimes. To avoid this problem, we choose $n \geqslant 3 \tau/\Delta t$.

Experimental

The flash photolysis apparatus utilized a Q-switched frequency-doubled ruby laser (Holobeam, Model 600) for excitation and a pulsed xenon lamp as measuring source. Triplet and radical species were followed at appropriate wavelengths with a monochromator and fast photomultiplier photometer, whose output was read either on an oscilloscope or broad-band digital transient recorder (Biomation, Model 8100). All computations described in this paper were carried out on a Hewlett-Packard calculator (Model 9821A). A more complete description of the apparatus will be published elsewhere [4].

Acknowledgement

Appendix

The algorithm presented as eqn. (1) is heuristically derived from knowledge of the solutions for unimolecular and bimolecular behavior. It closely

fits the assumed kinetics in simulated situations (see below), gives the correct solutions in the appropriate limits and successfully treats experimental data over a wide lifetime range (Fig. 3).

Consider that the time resolved concentration profile of product R is divided into channels of equal width Δt. R_0 is set equal to zero and R_1 is the concentration of R formed during the interval Δt between channels 0 and 1,

$$R_0 = 0 \tag{A1}$$

$$R_1 = \alpha T_0 (1 - e^{-k_1 \Delta t}) \tag{A2}$$

R_2 is given by the sum of R formed during the interval Δt between channels 1 and 2 and the amount of R remaining from channel 1 after undergoing bimolecular decay for a time Δt,

$$R_2 = \alpha T_0 (1 - e^{-2k_1 \Delta t}) - \alpha T_0 (1 - e^{-k_1 \Delta t}) + R_1/(1 + R_1 k_2 \Delta t) \tag{A3}$$

Combining the first two terms of eqn. (A3), the general expression eqn. (1) can be generated. Equation (4) may be reformulated in terms of a recursion relationship:

$$\Delta D_n = \Delta D_{n-1}^T \gamma + \beta_{n-1}(1 - \gamma) + \Delta D_{n-1}^R/(1 + \Delta D_{n-1}^R k_2' \Delta t) \tag{A4}$$

in which:

$$n \geqslant 1; \Delta D_0 = \Delta D_0^T; \gamma = e^{-k_1 \Delta t}; \beta_n = \beta_{n-1}\gamma; \beta_0 = \Delta D_\infty^R$$

The first term of eqn. (A4) gives the triplet contribution to ΔD_n and the last terms give the R contribution. Use of eqn. (A4) results in a considerable saving of computer time as the exponential term γ need be calculated only once for each variation of k_1 in the search procedure.

The closeness of fit of the algorithm to the kinetic situation considered here was tested by comparison with numerical integration of the rate equation for the radical product. For this purpose, we write, in the notation of eqn. (1):

$$\frac{dR}{dt} = k_R BT - k_2 R^2$$

$$= k_1 T_0 e^{-k_1 t} - k_2 R^2$$

This equation was solved by the Runge–Kutta procedure to obtain the transient absorbance, $\Delta D(t)$ relative to ΔD_0, for the simulated conditions of Fig. 1. Equation (4) was applied to the same set of parameters, using Δt values from 0.5 to 0.05 μs. The results are compared in Table 1A for the case (Fig. 1a) where "$\tau_{1/2}$" = 10 μs, representing a situation where ΔD_{max} is substantially below ΔD_∞. It is seen (Table 1A) that the algorithm yields systematically higher values for $\Delta D(t)$ than careful numerical integration, but even at the coarsest Δt interval (0.5 μs) the maximum error is less than 2%. At Δt = 0.05 μs, the algorithm checks to better than 0.2% everywhere along the curve. A similar fit is obtained for the situation in Fig. 1(b) ("$\tau_{1/2}$" = 10 μs), where the transient maximum occurs at ΔD_0. For the extreme case of "$\tau_{1/2}$" =

TABLE 1A

Algorithm fit to kinetic equations[a].

Time after flash (μs)	$\Delta D(t)/\Delta D_0$		
	Numerical[b] integration	Algorithm, with Δt	
		0.05 μs	0.5 μs
0	1.000	1.000	1.000
1	1.600	1.601	1.617
2	1.727	1.729	1.757
3	1.681	1.683	1.713
4	1.584	1.586	1.614
6	1.382	1.384	1.406
8	1.217	1.218	1.235
10	1.085	1.086	1.099

[a]Conditions as in Fig. 1(a), for "$\tau_{1/2}$" = 10 μs
($T_0 = 10^{-5} M$; $\Delta D_0 = 0.05$).
[b]By Runge–Kutta method. Step intervals of 0.1 μs and 0.01 μs gave same results.

5 μs, the algorithm error is about 50% larger than the example of Table 1A. Thus, at $\Delta t = 0.05$ μs, the maximum error is negligible, and is still less than 3% at the coarsest Δt interval (0.5 μs).

Finally, the algorithm was tested for its ability to extract k_1 and ΔD_∞ from the simulated "data" (Fig. 1(a), $\tau_{1/2}$ = 10 μs) obtained by numerical integration. To represent a typical case, a Δt interval of 0.2 μs and 20 "data points" over a 4 μs period were used, and the initial estimates of the parameters were taken to lie just within the first coarse grid spacing ($k_1 \pm 37\%$; $\Delta D_\infty \pm 8.5\%$). Under these conditions, the search procedure gave $k_1 = 0.97 \times 10^6$ and $\Delta D_\infty/\Delta D_0 = 2.002$, to be compared with the correct values, 1.00×10^6 and 2.000 respectively. Taking more points and a finer Δt interval improves the fit.

References

1 R. Bensasson and E. J. Land, Trans. Faraday Soc., 67 (1971) 1904.
2 L. Lindqvist, Arkiv. Kemi, 16 (1960) 79.
3 H. Linschitz and L. Pekkarinen, J. Am. Chem. Soc., 82 (1960) 2411.
4 L. J. Andrews, A. Deroulede and H. Linschitz, in press.